

A mathematical model for simulating respiratory control during support ventilation modes

Sebastian Larraza*. Nilanjan Dey**. Dan S. Karbing*. Morten Nygaard**.
Robert Winding**. Stephen E. Rees*

*Respiratory and critical care group (RCARE), Center for Model-based Medical Decision Support, Department of Health Science and Technology, Aalborg University, Aalborg, DK 9220, Denmark (Tel: +45-9940-9787; e-mail: larraza@hst.aau.dk).

**Department of Anaesthesia and Intensive Care, Regions Hospital Herning, Herning DK 7400, Denmark

Abstract: Mathematical model simulations may assist in the selection of mechanical ventilator settings. Previously, simulations have been limited to control ventilator modes, as these models lacked representation of respiratory control. This paper presents integration of a chemoreflex respiratory control model with models describing: ventilation and pulmonary gas exchange; oxygenation and acid-base status of blood; circulation; interstitial fluid and tissue buffering; and metabolism. A sensitivity analysis showed that typical response to changing ventilator settings can be described by base excess (BE), production of CO₂ ($\dot{V}CO_2$), and model parameters describing central chemoreceptor behavior. Since BE and $\dot{V}CO_2$, can be routinely measured, changes in ventilator support may therefore be used to identify patient-specific chemoreceptor drive, enabling patient-specific predictions of the response to changes in mechanical ventilation.

1. INTRODUCTION

Setting mechanical ventilation is a difficult and time-consuming process. Poor settings can increase the time spent on mechanical ventilation, and the risk of lung injury and mortality (Arnal *et al.*, 2012). Consequently, Decision Support Systems (DSS) have been developed to advise upon or automate the selection of mechanical ventilator settings (Tehrani and Roum, 2008a). These include rule-based systems such as the commercially-available SmartCare and Adaptive Support Ventilation (ASV) systems. SmartCare has been shown to be effective for managing pressure support ventilation to keep the end tidal partial pressure of CO₂ (PETCO₂) and respiratory frequency (fR) within a comfort zone (Lellouche *et al.*, 2006), and ASV has been shown appropriate for selecting ventilator settings that minimize the inspiratory work of breathing (Iotti *et al.*, 2010). Research systems have also been developed based upon mathematical physiological models rather than rules, these including SOPAVent (Wang *et al.*, 2010), Flex (Tehrani and Roum, 2008b) and the Intelligent Ventilator (INVENT) project (Rees, 2011). The potential advantage of such systems is that the physiological models can be tuned to the individual patient and used to simulate the patient's response to changes in mechanical ventilation, a useful process when selecting optimal ventilator settings.

To develop a model-based DSS for selecting optimal mechanical ventilator settings requires mathematical models of: 1) ventilation and pulmonary gas exchange; 2) oxygenation and acid-base status of blood; 3) circulation; 4) metabolism and 5) respiratory control. Using such models it should be possible to simulate the effects of changes in mechanical ventilation combined with the effects of, for example: changes in CO₂ production ($\dot{V}CO_2$) or O₂ consumption ($\dot{V}O_2$);

metabolic acidosis or alkalosis; impairment of gas exchange; and changes in respiratory drive due to sedation. The DSS INVENT includes all of these model components with the exception of a model of respiratory control (Rees, 2011). The absence of a model of respiratory control limits its use to fully sedated patients in controlled ventilator modes. As these patients represent only a small fraction presenting in the ICU, further development of the system to include a model of respiratory control is essential if the system is to have routine clinical application.

This paper presents the integration of a mathematical model of respiratory control (Duffin, 2005; Ainslie and Duffin, 2009) into the current INVENT set of models. The integrated model of respiratory control needs to be a) sufficiently complex to represent physiology adequately, and b) sufficiently simple to be tuned to the individual patient from routinely available clinical data. Accordingly, the paper has two objectives: 1) to postulate which respiratory control model parameters can be identifiable from patient data; and 2) to evaluate whether the model is sufficiently complex by exploring its ability to simulate the respiratory response to changes in ventilator support considering different levels of $\dot{V}CO_2$ and different blood acid-base states, represented by arterial base excess (BEa).

2. METHODS

2.1 Model description and calibration

Figure 1 illustrates the set of mathematical model components of INVENT including the mathematical representation of respiratory control. Figure 1A illustrates the structure of the model of ventilation and pulmonary gas exchange. This model has previously been shown to be identifiable from clinical data

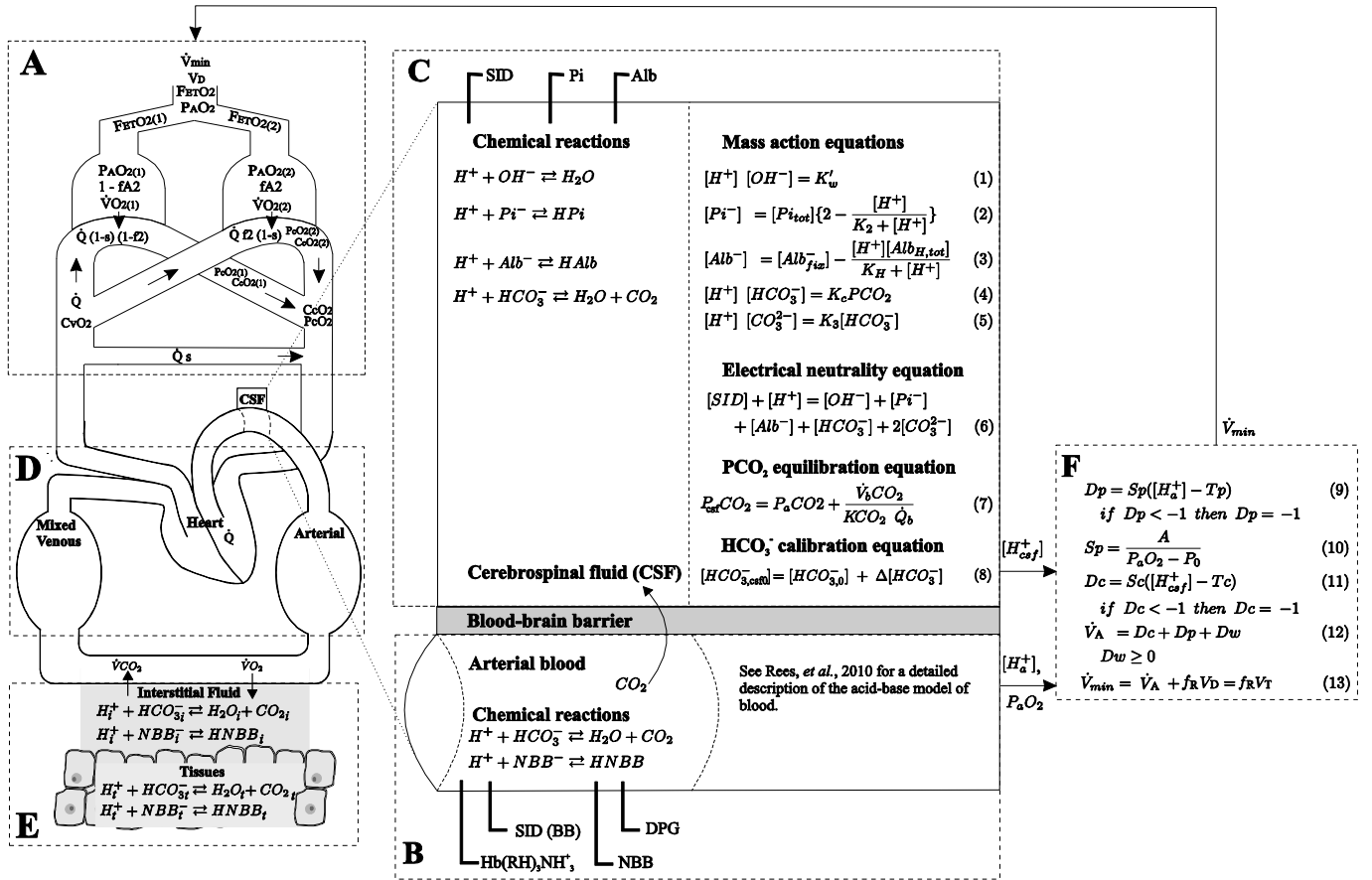


Fig. 1. Structure of the integrated model of respiratory control. The model includes sub-models of: ventilation and pulmonary gas exchange (A); oxygenation and acid-base status of blood (B); acid-base status of CSF (C); cardiac output, arterial and mixed venous pools (D); interstitial fluid and tissue buffering, and metabolism (E); and chemoreflex respiratory control (F).

on the variation of FIO_2 , and has been used to describe changes in gas exchange in numerous clinical situations (Karbing *et al.*, 2007; Karbing *et al.*, 2011). Figure 1B illustrates the structure of the model of oxygenation and blood acid-base status. This model has been shown to accurately describe the addition or removal of O_2 , CO_2 or strong acid to blood and also to describe the mixing of different blood samples (Rees *et al.*, 2010).

Figure 1C describes Duffin's model of cerebrospinal fluid (CSF) acid-base with the model constants listed in table 1. This model incorporates Stewart's and Watson's mass-action equations describing water, phosphate and albumin dissociation (1-3), formation of bicarbonate and carbonate (4-5), and electrical neutrality (6) (Duffin, 2005). In addition, the partial pressure of CO_2 in CSF ($P_{csf}CO_2$) is set equivalent to that in arterial blood (P_aCO_2) plus an increase due to the brain production of CO_2 (\dot{V}_bCO_2) (7) (Anslie and Duffin, 2009). Equation (8) is an addition to Duffin's model which permits CSF bicarbonate ($[HCO_3^-]_{csf}$) to be identifiable from steady state mixed venous bicarbonate ($[HCO_3^-]_b$), and therefore, consider conditions where blood bicarbonate, and base excess (BE) are altered; such as metabolic acidosis where blood bicarbonate and BE are reduced, or metabolic alkalosis where bicarbonate and BE are increased. $[HCO_3^-]_{csf}$ is calibrated to $[HCO_3^-]_b$ with a correction factor ($\Delta[HCO_3^-]$) being added to ensure that at normal conditions $[HCO_3^-]_{csf}$ is consistent with the normal value of SID_{csf} (31 mmol l^{-1}) reported by Duffin (2005). Determining $[HCO_3^-]_{csf}$ considering individual

patient conditions, e.g. metabolic acidosis or metabolic alkalosis, is important to estimate the CSF strong ion difference (SID_{csf}) by solving simultaneously (1-7). The estimated SID_{csf} is then assumed to be constant until blood reaches a different steady state due to the blood-brain barrier ability to constrain ion exchange.

The model illustrated in Figure 1 includes compartments representing CO_2 transport and storage including the arterial and venous compartments, and circulation represented as cardiac output (\dot{Q}) (Figure 1D). Figure 1E shows the model of interstitial fluid and tissue buffering, and metabolism included in the system (Andreassen and Rees, 2005). This model includes the bicarbonate and non-bicarbonate buffers in these relatively large volumes, \dot{V}_{O_2} and \dot{V}_{CO_2} . Figure 1F illustrates the model of respiratory control (9-12), with small adaptations and calibrations necessary for integration with the other models described as follows. The peripheral drive (Dp) is a linear function of the difference between the arterial hydrogen ion concentration ($[H^+]_a$) and the peripheral threshold (Tp) (9). The slope of this function is the sensitivity of the peripheral chemoreceptors (Sp), which is modulated by P_aO_2 as described by (10). Dp is allowed to have negative values up to $-1 l \text{ min}^{-1}$. In this way, the model includes an offset to allow disfacilitation of peripheral drive when $[H^+]_a$ falls below Tp , as suggested previously (Mohan and Duffin, 1997; Ursino *et al.*, 2001; Day and Wilson, 2008). The central drive (Dc) is a linear function of the difference between the CSF hydrogen

ion concentration ($[H^{+}csf]$) and the central threshold (T_c) (10). The slope of this function is the sensitivity of central chemoreceptors (Sc). Similarly, the function is allowed to have negative values up to -1 l min^{-1} to allow disfacilitation of D_c . The model of respiratory control includes two constants, with values previously specified by Duffin (2005) to be $A=2.373 \text{ l kPa (min nM l}^{-1})^{-1}$ and $P_0=4 \text{ kPa}$ to describe O_2 modulation of Sp . This model includes five parameters, two chemoreceptor sensitivities (Sp , Sc), two chemoreceptor thresholds (T_c , T_p), and wakefulness drive (D_w).

Equation (12) describes the alveolar ventilation (\dot{V}_A) as the sum of the two chemoreflex drives and wakefulness drive (D_w). D_w is the behavioral component of ventilation, and is considered independent of the chemoreflex respiratory control, but dependent on state of conscious. $D_w=0 \text{ l min}^{-1}$ represents unconscious breathing, and $D_w=2 \text{ l min}^{-1}$ is assumed to represent normal conditions during relaxed mechanical ventilation and conscious breathing. This value of D_w is lower than that reported by Duffin (2005), implying that D_w is not the major drive of spontaneous ventilation in mechanically ventilated patients. A value of $D_w=2 \text{ l min}^{-1}$, in combination with disfacilitation of -1 l min^{-1} from both central and peripheral drives also allows the simulation of apnea. Equation (13) describes the minute ventilation (\dot{V}_{min}) as \dot{V}_A plus ventilation of the serial dead space (V_D) that is equal to the product of tidal volume (V_T) and f_R .

The model components B, D and E in Figure 1, plus a single ventilated compartmental model of the lung have been previously coupled and implemented to simulate both dynamic and steady state conditions (Andreassen and Rees, 2005). The steady state model was modified adding extra state variables to account for alveolar concentration of O_2 and CO_2 in each of the ventilated compartments in Figure 1 ($F_{ETO_2(c1)}$, $F_{ETO_2(c2)}$, $F_{ETCO_2(c1)}$, $F_{ETCO_2(c2)}$). The inclusion of CSF and respiratory control components (Figures 1C and 1F) did not require the addition of any extra state variables as CO_2 changes in the CSF are assumed instantaneous, and SID_{csf} is estimated with $[HCO_{3,0}^-]$ at the start of simulations.

The integrated model, illustrated in Figure 1, is used to simulate steady state \dot{V}_A by specifying values for end tidal gas fractions (F_{ETO_2} , F_{ETCO_2}), arterial blood acid-base and oxygenation status (pHa , $PaCO_2$, and PaO_2), and model constants and parameters from table 1. Then, assuming steady state conditions, all other values can be calculated via the steady state model (Rees and Andreassen, 2005).

Normal values of peripheral and central thresholds (T_p and T_c) can be calibrated to several conditions. Here it is chosen to calibrate the model so as to produce normal \dot{V}_A and normal values of blood acid-base status for $D_w=0 \text{ l min}^{-1}$, i.e. unconscious breathing. The value of Sc was taken from Duffin (2005), and the value of Sp was obtained from (10) assuming normal PaO_2 of 12.15 kPa .

Normal values of T_p and T_c were calculated in several steps. First, normal steady state values of arterial blood ($pHa=7.4$, $BEa=0 \text{ mmol l}^{-1}$, $PaCO_2=5.35 \text{ kPa}$ and $PaO_2=12.15 \text{ kPa}$) were used along with the CSF acid-base model (1-7) to calculate

Table 1. Parameters and constants of the integrated model components

CSF acid-base model constants		
Symbol	Name	Values
K_w	Ion product for water	2.39×10^{-14}
K_c	Combined CO_2 equilibrium and solubility	2.45×10^{-11}
K_3	Carbonate dissociation	1.16×10^{-10}
K_2	Phosphoric acid dissociation constant	2.19×10^{-7}
K_H	Histidine dissociation constant	1.77×10^{-7}
K_{CO_2}	CO_2 Dissociation constant ($ml (ml \text{ kPa})^{-1}$)	0.0375
$[Alb^{Fix}]$	Albumin fixed negative charge concentration ($mM l^{-1}$)	3.95
$[Alb^{H, tot}]$	Albumin concentration of histidine residues ($mM l^{-1}$)	3.01
$[Pi_{tot}]$	Phosphate concentration ($mM l^{-1}$)	0.61
\dot{V}_{bCO_2}	Brain production of CO_2 ($ml (min 100gr)^{-1}$)	3
\dot{Q}_b	Brain blood flow ($ml (min 100g)^{-1}$)	55
$\Delta[HCO_3^-]$	CSF bicarbonate calibration factor ($mmol l^{-1}$)	0.12
Respiratory control model parameters		
Symbol	Name	Normal values
Sc	Central sensitivity ($l \text{ min}^{-1} (nmol l^{-1})^{-1}$)	1.78
Sp	Peripheral sensitivity ($l \text{ min}^{-1} (nmol l^{-1})^{-1}$)	0.29
T_c	Central threshold ($nmol l^{-1}$)	45.24
T_p	Peripheral threshold ($nmol l^{-1}$)	37.75
D_w	Wakefulness drive ($l \text{ min}^{-1}$)	2
Blood acid-base, interstitial fluid and tissue buffering models constants		
Symbol	Name	Normal values
Hb	Hemoglobin concentration ($mmol l^{-1}$)	9.3
$tNBB$	Total non-bicarbonate buffer base concentration ($mmol l^{-1}$)	23.5
\dot{Q}	Cardiac output ($l \text{ min}^{-1}$)	5
\dot{V}_{CO_2}	CO_2 production ($mmol \text{ min}^{-1}$)	9.23
\dot{V}_{O_2}	O_2 consumption ($mmol \text{ min}^{-1}$)	10.5
V_{blood}	Blood volume (l)	4.5
V_{int}	Interstitial fluid volume (l)	9.5
V_{tiss}	Tissue volume (l)	14
Pulmonary gas exchange model parameters		
Symbol	Name	Normal values
s	Pulmonary shunt (%)	5
f_2	Fraction of non-shunted perfusion to compartment 2	0.9
f_{A2}	Fraction of alveolar ventilation to compartment 2	0.9
V_d	Serial dead space (l)	0.15

$[H^{+}csf]$. Second, values of $[H^{+}a]$, $[H^{+}csf]$ and normal $\dot{V}_A=4.2 \text{ l min}^{-1}$ were then inserted into (9, 11 and 12) with these equations being solved simultaneously to calculate T_c and T_p . This situation represents calculation of 4 unknowns (D_p , D_c , T_p , T_c) from 3 equations and it was therefore necessary to make an assumption. Third, we assumed that under normal conditions the difference between $[H^{+}]$ and threshold values would be the same for both blood and CSF, i.e. $([H^{+}a]-T_p) = ([H^{+}csf]-T_c)$. The calculated normal values were $T_p=37.75 \text{ nmol l}^{-1}$ and $T_c=45.24 \text{ nmol l}^{-1}$.

2.2 Simulating patient specific response to changes in ventilator support

For the integrated model to be clinically useful it should be able to be tuned to reflect the individual patient's response to changes in ventilator support. Model tuning should be possible

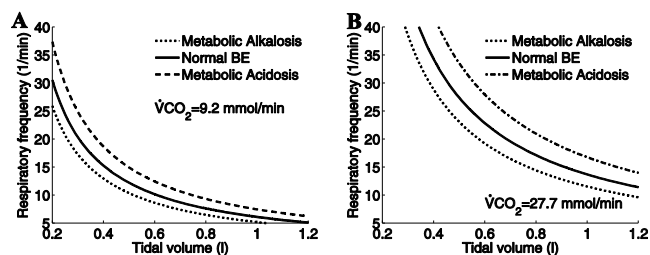


Fig. 2. Sensitivity analysis of respiratory response to changes in measured factors. Plots of simulated fR response to changes in ventilator support (VT) for different acid-base conditions and $\dot{V}CO_2$ levels. (A) Simulated fR for three acid-base conditions and normal $\dot{V}CO_2$. (B) Simulated fR for three acid-base conditions and increased $\dot{V}CO_2$.

from routinely available clinical data collected under the relevant clinical scenario, i.e. reducing pressure or volume support.

Reduction in ventilatory support (e.g. reduction in VT) will typically result in an increase in fR and hence a constant $\dot{V}A$ so as to maintain pHa within normal range. This pattern of reducing ventilatory support and increasing fR will depend for the individual patient upon two sets of factors, those which are directly measured such as acid-base status and metabolism (BEa and $\dot{V}CO_2$), and those which are not, i.e. the individual patient's pulmonary gas exchange parameters (s, fA2 and f2) and chemoreflex response parameters (Sp, Sc, Tp, Tc). Therefore, two sensitivity analyses are performed here: 1) evaluation of model simulations to changes in measured factors (BEa and $\dot{V}CO_2$); and 2) evaluation of model simulations to changes in chemoreflex response parameters (Sp, Sc, Tp, Tc). All sensitivity analysis simulations were performed assuming normal values for pulmonary gas exchange parameters. The details of these analyses are given below.

2.2.1 Evaluation of model simulations to changes in measured factors (BEa and $\dot{V}CO_2$)

The integrated model was used to simulate changes in ventilator support at different acid-base and metabolism in normal chemoreflex conditions. To explore the integrated model's behavior to different values of acid-base and $\dot{V}CO_2$, changes in fR were simulated on modifying VT in the range 200 to 1200 ml. Steady state values of fR were simulated for three acid-base conditions of blood: normal BEa (BEa=0.1 mmol l⁻¹), metabolic acidosis (BEa=-4.2 mmol l⁻¹) and metabolic alkalosis (BEa=5.3 mmol l⁻¹); at two $\dot{V}CO_2$ levels (9.2 and 27.7 mmol min⁻¹).

2.2.2 Evaluation of model simulations to changes in chemoreflex response parameters (Sc, Sp, Tc and Tp)

To explore the integrated model's behavior to different values of chemoreflex model parameters, changes in fR were simulated on modifying VT in the range 200 to 1200 ml. Steady state values of fR were simulated for different values of model parameters Sc, Tc, Sp and Tp. These simulations

were performed in three conditions: 1) normal values of BEa and $\dot{V}CO_2$ (BEa=0.1 mmol l⁻¹ and $\dot{V}CO_2$ =9.2 mmol l⁻¹); 2) normal BEa but increased $\dot{V}CO_2$ (BEa=0.1 mmol l⁻¹ and $\dot{V}CO_2$ =27.7 mmol l⁻¹); and 3) decreased BEa (metabolic acidosis) and increased $\dot{V}CO_2$ (BEa=-4.2 mmol l⁻¹ and $\dot{V}CO_2$ =9.2 mmol l⁻¹). With the last two representing conditions that augment the respiratory drive. In this way, the effect of the individual parameters could be shown as well as their interaction with the measured factors. To perform these simulations, model parameters were modified one at a time and keeping the remaining with normal values. Sensitivities (Sc and Sp) were varied by multiplying normal values by zero and two. Thresholds (Tc and Tp) were varied by adding or subtracting 5 nmol l⁻¹ to normal values.

3. RESULTS

3.1 Evaluation of model simulations to changes in measured factors (BEa and $\dot{V}CO_2$)

Figure 2 illustrates simulations of the respiratory response to changes in VT for different values of measured factors BEa and $\dot{V}CO_2$. Figure 2A illustrates the effects of high and low BEa at normal $\dot{V}CO_2$, showing that metabolic alkalosis (high BEa) suppresses and metabolic acidosis (low BEa) augments respiratory drive. Figure 2B illustrates the effects of high and low BEa, at a high value of $\dot{V}CO_2$, showing that these effects act in combination such that for high $\dot{V}CO_2$ all curves are shifted and respiratory drive augmented.

3.2 Evaluation of model simulations to changes in chemoreflex response parameters (Sc, Sp, Tc, and Tp)

Figure 3 illustrates simulations of the respiratory response to changes in VT for different values of non-measured factors, i.e. chemoreflex model parameters, at 3 conditions: normal BEa and normal $\dot{V}CO_2$; normal BEa and increased $\dot{V}CO_2$; and metabolic acidosis and increased $\dot{V}CO_2$. Plots are arranged in 3 columns and 2 rows; each column corresponding to the first, second and third conditions, and each row corresponding to changes in chemoreflex parameters Sc and Tc respectively. Solid lines represent simulations with normal parameter values with these lines systematically shifted for increased $\dot{V}CO_2$ or for the combination of increased $\dot{V}CO_2$ and decreased BEa, as also shown in Figure 2.

The first row of Figure 3 presents simulations of the respiratory response to changes in VT for different values of Sc. Figures 3A, 3B and 3C show that decreasing Sc suppresses and increasing Sc augments the respiratory drive, with a greater sensitivity to reducing Sc. The sensitivity of the respiratory response to changes in Sc is greater for increased $\dot{V}CO_2$ and the combination of increased $\dot{V}CO_2$ and decreased BEa.

The second row of Figure 3 presents simulations of the respiratory response to changes in VT for different values of Tc. Figures 3D, 3E and 3F show that decreasing Tc augments and increasing Tc suppress the respiratory drive. The sensitivity of the respiratory response to changes in Tc is greater for increased $\dot{V}CO_2$ and the combination of increased

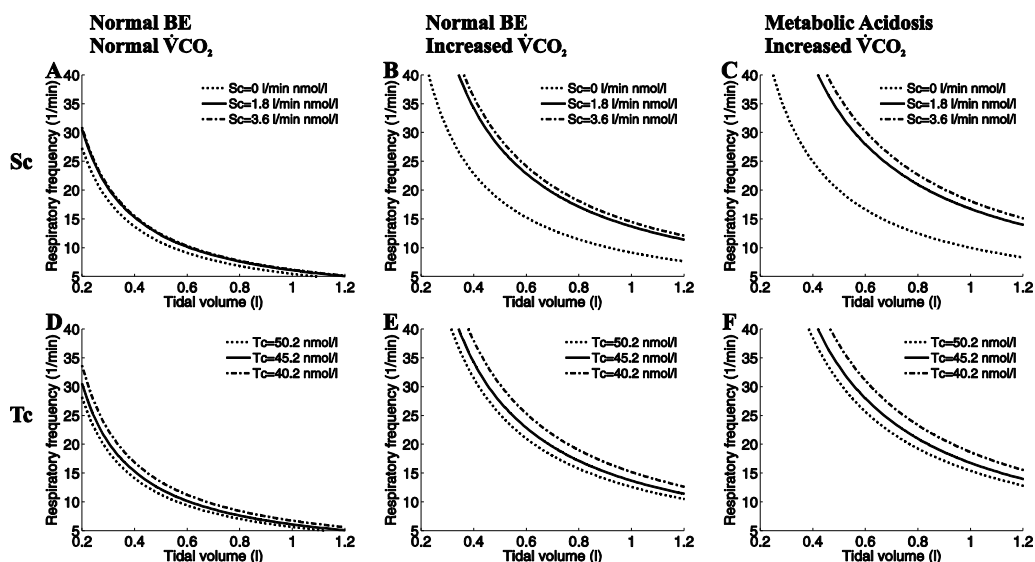


Fig. 3. Sensitivity analysis of respiratory response to changes in chemoreflex model parameters. Plots of simulated fR response to changes in ventilation support (VT) for 3 different sets of measured factors: normal BEa and normal $\dot{V}CO_2$, (A, D); normal BEa and increased $\dot{V}CO_2$ (B, E); and decreased BEa and increased $\dot{V}CO_2$ (C, F). Solid lines represent simulated fR response using normal chemoreflex model parameter values. Dotted and dashed lines represent simulated fR response with variation of parameter Sc (A, B, C) and Tc (D, E, F).

$\dot{V}CO_2$ and decreased BEa. The normal respiratory response is unaffected due to changes in values of Sp and Tp respectively in the situation of normal oxygenation (not shown).

4. DISCUSSION

This paper describes the integration of a mathematical model of chemoreflex respiratory control with models describing ventilation and pulmonary gas exchange, oxygenation and acid-base of blood, circulation, interstitial fluid and tissue buffering, and metabolism. The purpose of this integrated model is to be part of a DSS, providing advice on appropriate mechanical ventilation in support ventilation modes. In these ventilation modes pressure or volume support is determined by the clinician and set on the ventilator, with the patient responding in terms of fR dependent upon their individual physiological status. For mathematical models to be useful in aiding this decision they need to be complex enough to describe this individual response, and simple enough to be parameterized or tuned to the individual patient from routinely available clinical data.

The integrated model in Figure 1 includes a representation of the CSF acid-base and a chemoreflex model of respiratory control, which enable the simulation of the respiratory drive for alterations in the underlying steady state BEa and $\dot{V}CO_2$. To do so, Duffin's model was modified to allow simulations of: respiratory response due to metabolic acidosis or alkalosis via the SIDcsf; and disfacilitation of Dc and Dp . Disturbances in the SIDcsf alter the central chemoreceptor signaling [H^+ csf] and hence, the respiratory drive (Lahiri and Forster, 2003).

The balance between model simplicity and complexity necessitates a number of model assumptions in relation to the chemoreflex component. The CSF acid-base status is estimated using the model in figure 1C (Duffin, 2005), assuming that O_2 and CO_2 molecules cross freely across the blood brain barrier. It is also assumed that there is no (short

term) electrolyte exchange between blood and CSF such that when SIDcsf is calibrated to initial venous blood bicarbonate values ($[HCO^-_{3,0}]$), then SIDcsf remains fixed when simulating respiratory changes.

To our knowledge, this is the first time that a chemoreflex model has been integrated with models describing ventilation and pulmonary gas exchange, oxygenation and acid-base status of blood, circulation, interstitial fluid and tissue buffering, and metabolism for simulating the respiratory response to changes in mechanical ventilation for severely ill patients. Several other models have simulated respiratory control (for example: Ursino *et al.*, 2001; Aittokallio *et al.*, 2006, Duffin, 2010), however, these models have focused upon breathing pattern, and response to hypercapnia and hypoxia. In the context of mechanical ventilation, model complexity may be constrained to simulating steady state response to changes in ventilator support.

Inclusion of the previous models of INVENT are also important. The model of ventilation and pulmonary gas exchange is identifiable for the individual patient, allowing identification of pulmonary shunt, low \dot{V}/\dot{Q} and high \dot{V}/\dot{Q} (Karbing *et al.*, 2011). The blood acid-base model has been shown to simulate blood mixing accurately and includes consideration of the Bohr-Haldane effect, which is important in patients where pHa may be far from normal. In addition, the incorporation of an explicit compartment for interstitial fluid and tissue buffering, enables simulation of bicarbonate distribution between blood and interstitial fluid which is critical to correct simulation of in-vivo arterial CO_2 levels (Andreassen and Rees, 2005).

The integrated model assumes constant cardiac output (\dot{Q}) and constant cerebral blood flow (CBF). In principle, \dot{Q} and CBF increase as a function of $PaCO_2$. Increased CBF washes out CO_2 from the CSF compartment (Mohan and Duffin, 1997;

Ainslie and Duffin, 2009; Duffin, 2010). Although CBF increases during hypercapnia, the CBF effects on ventilation sensitivity to CO₂ are negligible (Ursino *et al.*, 2001), and not fully understood (Pandit *et al.*, 2007). Separation of the effects of CBF cannot be identified from the data describing changes in ventilator volume support, meaning that this level of complexity would not be helpful.

In conclusion, this paper has described the integration of Duffin's chemoreflex model into a set of physiological models. In doing so, it has been shown that the integrated model is sensitive to measured factors (BE_a and $\dot{V}CO_2$), and non-measured factors describing the central chemoreflex drive under conditions of normal pulmonary gas exchange and oxygenation. Central chemoreflex parameters SID_{csf}, T_c and S_c may be identifiable from BE_a, $\dot{V}CO_2$, and measured respiratory response to changes in ventilation support. Therefore identifying patient-specific chemoreflex drive, potentially enables the simulation of respiratory response to changes in ventilation support. Further evaluation of the integrated model with patient data including pulmonary gas exchange, acid-base status and metabolic abnormalities is required.

ACKNOWLEDGEMENTS

We thank James Duffin, Ph. D. for his comments on the manuscript.

REFERENCES

- Ainslie, P. and J. Duffin (2009). Integration of cerebrovascular CO₂ reactivity and chemoreflex control of breathing: mechanisms of regulation, measurement and interpretation. *Am J Physiol Regul Integr Comp Physiol*, **296**, R1473-R1495.
- Aittokallio, T., M. Gyllenberg, O. Polo, J. Toivonen, and A. Virkki, (2006). Model-Based Analysis of Mechanisms Responsible for Sleep-Induced Carbon Dioxide Differences. *Bull. Math. Biol.*, **68**, 315-341.
- Andreassen, S. and S.E. Rees (2005). Mathematical Models of Oxygen and Carbon Dioxide Storage and Transport: Interstitial Fluid and Tissue Stores and Whole-Body Transport. *Crit Rev Biomed Eng*, **33**, 265-298.
- Arnal, J.M., M. Wysocki, D. Novotni, D. Demory, R. Lopez, S. Donati, I. Garnier, G. Corno, and J. Durand-Gasselin (2012). Safety and efficacy of a fully closed-loop control ventilation (IntelliVent-ASV) in sedated ICU patients with acute respiratory failure: a prospective randomized crossover study. *Intensive Care Med*, **38**, 781-787.
- Day, T.A. and R.J.A. Wilson (2008). 78. A Negative Interaction Between Central and Peripheral Respiratory Chemoreceptors May Underlie Sleep-Induced Respiratory Instability: A Novel Hypothesis. In: *Integration in Respiratory Control: From Genes to Systems*. (Poulin M.A. and R.J.A. Wilson (Eds)) 447-451. Springer, New York.
- Duffin, J. (2005). Role of acid-base balance in the chemoreflex control of breathing. *J. Appl. Physiol.*, **99**, 2255-2265.
- Duffin, J. (2010). The role of the central chemoreceptors: A modeling perspective. *Respir. Physiol. Neurobiol.*, **173**, 230-243.
- Iotti, G.A., A. Polito, M. Belliato, D. Pasero, G. Beduneau, M. Wysocki, J.X. Brunner, A. Braschi, L. Brochard, J. Mancebo, V.M. Ranieri, J.C.M. Richard, and A.S. Slutsky, (2010). Adaptive support ventilation versus conventional ventilation for total ventilatory support in acute respiratory failure. *Intensive Care Med*, **36**, 1371-1379.
- Karbing, D.S., S. Kjaergaard, B.W. Smith, K. Espersen, C. Allerod, S. Andreassen, and S.E. Rees (2007). Variation in the PaO₂/FiO₂ ratio with FiO₂: mathematical and experimental description, and clinical relevance. *Crit Care*, **11**, R118-R124.
- Karbing, D.S., S. Kjaergaard, K. Espersen, and S.E. Rees (2011). Minimal model quantification of pulmonary gas exchange in intensive care patients. *Med Eng Phys*, **33**, 240-248.
- Lahiri, S. and R.E.I. Forster (2003). CO₂/H⁺ sensing: peripheral and central chemoreception. *Int. J. Biochem. Cell Biol.*, **35**, 1413-1435.
- Lellouche, F., J. Mancebo, P. Joillet, J. Roeseler, F. Schortgen, M. Dojat, B. Cabello, L. Bouadma, P. Rodriguez, S. Maggiore, M. Reynaert, S. Mersmann, and L. Brochard (2006). A Multicenter Randomized Trial of Competent-driven protocolized Weaning from Mechanical Ventilation. *Am. J. Respir. Crit. Care Med.*, **174**, 894-900.
- Mohan, R., and J. Duffin (1997). The effect of hypoxia on the ventilatory response to carbon dioxide in man. *Respir Physiol*, **108**, 101-115.
- Pandit, J.J., R.M. Mohan, N.D. Paterson, and M.J. Poulin (2007). Cerebral blood flow sensitivities to CO₂ measured with steady-state and modified rebreathing methods. *Respir. Physiol. Neurobiol.*, **159**, 34-44.
- Rees, S.E. and S. Andreassen (2005). Mathematical Models of Oxygen and Carbon Dioxide Storage and Transport: The Acid-Base Chemistry of the Blood. *Crit Rev Biomed Eng*, **33**, 209-264.
- Rees, S.E., E. Klastrup, J. Handy, S. Andreassen, and S.R. Kristensen (2010). Mathematical modelling of the acid-base chemistry and oxygenation of blood: a mass balance, mass action approach including plasma and red blood cells. *Eur. J. Appl. Physiol.*, **108**, 483-494.
- Rees, S.E. (2011). The Intelligent Ventilator (INVENT) project: The role of mathematical models in translating physiological knowledge into clinical practice. *Comput Methods Programs Biomed*, **104S**, S1-S29.
- Tehrani, F.T. and J.H. Roum, (2008a). Intelligent decision support systems for mechanical ventilation. *Artificial Intelligence in Medicine*, **44**, 171-182.
- Tehrani, F.T. and J.H. Roum, (2008b). FLEX: a new computerized system for mechanical ventilation. *J Clin Monit Comput*, **22**, 121-139.
- Ursino, M., E. Magosso, and G. Avanzolini, (2001). An integrated model of the human ventilatory control system: the response to hypercapnia. *Clin Physiol*, **21**, 447-464.
- Wang, A., M. Mahfouf, G.H. Mills, G. Panoutsos, D.A. Linkens, K. Goode, H.F. Kwok, and M. Denai (2010). Intelligent model-based advisory system for management of ventilated intensive care patients Part II: Advisory system design and evaluation. *Comput Methods Programs Biomed*, **99**, 208-217.